



## The influence of head motion on intrinsic functional connectivity MRI

Koene R.A. Van Dijk<sup>a,b</sup>, Mert R. Sabuncu<sup>b,c</sup>, Randy L. Buckner<sup>a,b,d,e,\*</sup>

<sup>a</sup> Harvard University Department of Psychology, Center for Brain Science, Cambridge, MA, USA

<sup>b</sup> Athinoula A. Martinos Center for Biomedical Imaging, Department of Radiology, Massachusetts General Hospital, Charlestown, MA, USA

<sup>c</sup> Computer Science and Artificial Intelligence Lab, Massachusetts Institute of Technology, Cambridge, MA, USA

<sup>d</sup> Department of Psychiatry, Massachusetts General Hospital, Boston, MA, USA

<sup>e</sup> Howard Hughes Medical Institute, Cambridge, MA, USA

### ARTICLE INFO

#### Article history:

Received 29 April 2011

Revised 8 July 2011

Accepted 14 July 2011

Available online 23 July 2011

#### Keywords:

Functional MRI

BOLD

Connectome

Resting-state

Movement

### ABSTRACT

Functional connectivity MRI (fcMRI) has been widely applied to explore group and individual differences. A confounding factor is head motion. Children move more than adults, older adults more than younger adults, and patients more than controls. Head motion varies considerably among individuals within the same population. Here we explored the influence of head motion on fcMRI estimates. Mean head displacement, maximum head displacement, the number of micro movements (>0.1 mm), and head rotation were estimated in 1000 healthy, young adult subjects each scanned for two resting-state runs on matched 3T scanners. The majority of fcMRI variation across subjects was not linked to head motion. However, head motion had significant, systematic effects on fcMRI network measures. Head motion was associated with decreased functional coupling in the default and frontoparietal control networks – two networks characterized by coupling among distributed regions of association cortex. Other network measures increased with motion including estimates of local functional coupling and coupling between left and right motor regions – a region pair sometimes used as a control in studies to establish specificity. Comparisons between groups of individuals with subtly different levels of head motion yielded difference maps that could be mistaken for neuronal effects in other contexts. These effects are important to consider when interpreting variation between groups and across individuals.

© 2011 Elsevier Inc. All rights reserved.

### Introduction

Resting-state functional connectivity MRI (fcMRI) is widely used to explore the architecture of brain systems. Studies of differences across the lifespan, between individuals with clinical diagnoses, and across varied personality traits have become common (for recent reviews, see Fornito and Bullmore, 2010; Fox and Greicius, 2010; Vogel et al., 2010; Zhang and Raichle, 2010). The technique is robust and yields reliable measures within individuals (e.g., Honey et al., 2009; Meindl et al., 2010; Shehzad et al., 2009; Van Dijk et al., 2010; Zuo et al., 2010). Recent family and twin studies suggest functional connectivity estimates are heritable and thus may offer insight into how genetic variation affects brain function (Fornito et al., 2011; Glahn et al., 2010). However, there is general awareness that resting state fcMRI is sensitive to confounding factors including head motion even after common data preprocessing steps (Buckner, 2010; Cole et al., 2010). Head motion has long been known to be a confound in task-based functional MRI studies, but has become a particularly challenging problem in recent studies using fcMRI. Effects of interest

are often between groups of subjects where differences in motion are expected such as between children and young adults, between young and old adults, and between patients and controls. The present paper explores how head motion affects measures of functional connectivity.

### Methods

#### Overview

The primary focus of the paper is to explore how between-subject differences in head motion affect MRI measures of intrinsic functional connectivity. A large sample of data from typical, healthy control subjects ages 18 to 30 were selected ( $n = 1110$ ). All subjects were imaged on matched MRI scanners using the same MRI sequence. Subjects with artifacts or abnormally low temporal signal-to-noise (tSNR) were eliminated but otherwise the sample represents a typical convenience sample of good to excellent quality data. The movement properties of the remaining sample ( $n = 1088$ ) were characterized to illustrate the dispersion. Functional connectivity metrics were then estimated for 1000 subjects. Head motion was explored as a continuous variable to determine how it affected various functional connectivity metrics including correlation strength among regions

\* Corresponding author at: Harvard University, 52 Oxford Street, Northwest Building, 280.06, Cambridge, MA 02138, USA. Fax: +1 617 496 9385.

E-mail address: [randy\\_buckner@harvard.edu](mailto:randy_buckner@harvard.edu) (R.L. Buckner).

within the default network, the frontoparietal control network, the motor network, and for a measure of local functional coupling. Then, subjects were divided into 10 groups representing those individuals who moved the least (Group 1) to those individuals who moved the most (Group 10). Group difference maps were constructed to illustrate how differences can arise in functional connectivity analyses when the only known major difference between the groups is head motion. As a final analysis we explored whether between-subject differences in head motion are stable over time.

### Subjects

Paid participants were clinically normal young adults with normal or corrected-to-normal vision, without a history of neurological or psychiatric illness, and not taking any psychoactive medications ( $n=1110$ ). Subjects were excluded if artifacts were detected in the functional MRI data ( $n=2$ ) and when the tSNR from either of the two functional MRI runs was lower than 100 ( $n=20$ ). The movement properties of the remaining sample ( $n=1088$ ) were characterized to illustrate the distribution. The sample was divided into 10 bins representing those individuals who moved least (Group 1) to those individuals who moved most (Group 10) (Table 1). Subjects were randomly selected to form groups of 100 subjects with the only constraint that either a male or a female was removed, whichever made the groups most balanced in terms of sex. In these 1000 subjects (ages 18 to 30; mean age = 20.6 yr; 57% female; 88% right handed) functional connectivity was analyzed. Analysis of variance indicated that age was evenly distributed across motion groups ( $F(9, 990) = 1.14$ ,  $p = 0.33$ ), while sex was not ( $\chi^2(9, 1000) = 18.9$ ,  $p < 0.05$ ). For the results that follow it is important to note that Groups 1 and 10 differed significantly regarding sex distribution ( $\chi^2(1, 200) = 9.5$ ,  $p < 0.01$ ), while sex was equally distributed between Groups 3 and 8 ( $\chi^2(1, 200) = 0.02$ ,  $p = 0.89$ ) and Groups 5 and 6 ( $\chi^2(1, 200) = 0.08$ ,  $p = 0.77$ ). A total of 42 subjects (ages 18 to 26; mean age = 20.1 yr; 62% female) were scanned on two separate days within 1 year to provide a dataset amenable to test reliability. Participants provided written informed consent in accordance with guidelines set by institutional review boards of Harvard University and Partners Healthcare.

### MRI data acquisition

All data were collected on matched 3T Tim Trio scanners (Siemens, Erlangen, Germany) located at Harvard University and the Massachusetts General Hospital using the 12-channel phased-array head coil supplied by the vendor. The functional imaging data were acquired using a gradient-echo echo-planar imaging (EPI) sequence sensitive to blood oxygenation

level-dependent (BOLD) contrast (Kwong et al., 1992; Ogawa et al., 1992). Parameters were TR = 3000 ms, TE = 30 ms, flip angle = 85°,  $3 \times 3 \times 3$  mm voxels, FOV = 216 with 47 slices aligned to the anterior-commissure posterior-commissure (AC-PC) plane using automated alignment (Van der Kouwe et al., 2005). Two BOLD runs of 124 volumes each were acquired. Slice acquisition order was interleaved. Earplugs were used to attenuate scanner noise and head motion was restrained with a foam pillow and extendable padded head clamps. Before each resting state scan subjects were instructed to simply rest in the scanner with their eyes open while staying as still as possible. Structural data included a high-resolution multi-echo T1-weighted magnetization-prepared gradient-echo image (multi-echo MP-RAGE; Van der Kouwe et al., 2008). Further details of data acquisition can be found in Yeo et al. (2011).

### Functional MRI data preprocessing

Data processing was conducted as it would be for typical fMRI data analysis including correction for within-subject head motion. The first four volumes of each run were discarded to allow for T1-equilibration effects. Slice acquisition dependent time shifts were corrected per volume (SPM2, Wellcome Department of Cognitive Neurology, London, UK). Then, rigid body translation and rotation from each volume to the first volume were used to correct for head motion (Jenkinson et al., 2002, FMRIB, Oxford, UK). Atlas registration was achieved by computing affine and non-linear transforms connecting the first volume of the functional run using SPM2, with a BOLD EPI template in the Montreal Neurological Institute (MNI) atlas space (Evans et al., 1993). Data were resampled to 2-mm isotropic voxels and spatially smoothed using a 6-mm full-width half-maximum (FWHM) Gaussian kernel. Temporal (band-pass) filtering removed constant offsets and linear trends over each run while retaining frequencies below 0.08 Hz and the mean signal intensity over the run was removed.

Several sources of spurious or regionally nonspecific variance were removed by regression of nuisance variables including (i) six parameters obtained by rigid body head motion correction, (ii) the signal averaged over the whole brain (global signal), (iii) the signal averaged over the lateral ventricles, and (iv) the signal averaged over a region centered in the deep cerebral white matter. Temporally shifted versions of these waveforms were also removed by inclusion of the first temporal derivatives (computed by backward differences) in the linear model. This regression procedure removes variance unlikely to represent regionally specific correlations of neuronal origin. Regression of each of these signals was performed simultaneously and the residual volumes were retained for the fMRI analysis. See Vincent et al. (2006) and Van Dijk et al. (2010) for detailed descriptions of the above procedures.

### Measurement of head motion

Four separate metrics of head motion were calculated from the translation and rotation parameters from the rigid body correction of head motion (Jenkinson et al., 2002). The four metrics were: *Mean Motion*, *Maximum Motion*, *Number of Movements* and *Rotation*. Mean Motion represents the mean absolute displacement of each brain volume as compared to the previous volume and was estimated from the translation parameters in the x (left/right), y (anterior/posterior), and z (superior/inferior) directions. Maximum Motion was estimated as the maximum absolute translation of each brain volume as compared to the previous volume in x, y, and z directions. The mean and maximum displacements in 3D space for each brain volume were computed as the root-mean-square (RMS) of the translation parameters (displacement = square root ( $x^2 + y^2 + z^2$ )) and expressed in mm. Number of Movements was estimated as the number of relative displacements > 0.1 mm in 3D space between adjacent volumes. Thus, the metric is expressed as an integer with the minimum possible value being 0 and the maximum  $n - 1$  where  $n$  is the

**Table 1**  
Demographics and Mean Motion displacement of study participants.

Group	n	Mean age <sup>a</sup> (SD)	M/F <sup>b</sup>	Mean Motion in mm <sup>c</sup> (SD)
1	100	20.8 (2.4)	33/67	0.027 (0.002)
2	100	20.5 (2.3)	39/61	0.032 (0.001)
3	100	20.3 (2.2)	45/55	0.036 (0.001)
4	100	20.7 (2.5)	37/63	0.040 (0.001)
5	100	20.6 (2.1)	38/62	0.044 (0.001)
6	100	20.5 (2.4)	36/64	0.048 (0.001)
7	100	20.3 (2.1)	51/49	0.052 (0.002)
8	100	20.9 (2.8)	46/54	0.059 (0.003)
9	100	20.6 (2.4)	47/53	0.072 (0.005)
10	100	21.1 (2.5)	55/45	0.100 (0.021)
Total	1000	20.6 (2.4)	427/573	0.051 (0.004)

<sup>a</sup> Age was evenly distributed across groups.

<sup>b</sup> Sex distribution was significantly different across groups.

<sup>c</sup> Mean Motion = mean absolute displacement of each brain volume as compared to the previous volume.

number of acquired volumes in the study. Rotation was a single angle measurement based on Euler's rotation theorem that expresses any 3D rotation as a single angle and corresponding axis of rotation. Rotation was computed as the average of the absolute value of the Euler angle of the rotation of each brain volume as compared to the previous volume. The Euler angle can be computed using the following formula:  $\arccos((\cos(\phi)\cos(\theta) + \cos(\phi)\cos(\psi) + \cos(\theta)\cos(\psi) + \sin(\phi)\sin(\psi)\sin(\theta) - 1)/2)$ , where  $\phi$ ,  $\theta$ , and  $\psi$  are the rotational parameters around the three axes. For most analyses, we used Mean Motion as the central metric of head motion but, as will be noted, use of other metrics does not significantly change the results.

#### Measurement of temporal signal-to-noise ratio (tSNR)

tSNR was computed for each of the two resting-state functional runs and used as another estimate of data quality. We have found that tSNR using slice estimates is a good predictor of data quality and low values identify subjects with high head motion or other causes of data instability. Here we formally explored the relation of tSNR to motion. For each subject, an inclusive brain mask was estimated that included signal values  $>150$ . The mean signal across the BOLD run (exclusive of the first four volumes during which T1-stabilization occurred) was calculated for each slice, and then the mean value was divided by the standard deviation of the signal intensity within the slice over time. The mean tSNR value across all voxels in the brain mask served as the measure of tSNR for the BOLD fMRI data.

#### Functional connectivity analysis

Four functional connectivity metrics were calculated targeting the *default network*, the *frontoparietal control network*, the *motor network*, and *local functional coupling*. For the three networks, Pearson's correlation coefficients were computed between time courses that were extracted from a priori spherical regions of interest (ROIs) within each network. Fisher's *r*-to-*z* transformation (Zar, 1996) was applied to each correlation coefficient in order to increase normality of the distribution of correlation values. Functional connectivity was then averaged across all pairs of regions within the network to form a single composite metric of functional connectivity strength. Regions forming the default network (Raichle et al., 2001) were based on Van Dijk et al. (2010) and included the posterior cingulate cortex (pCC: 0, -53, 26), medial prefrontal cortex (0, 54, -4), and left and right inferior parietal lobule (-46, -48, 36 and 50, -62, 32). Regions forming the frontoparietal control network were based on Vincent et al. (2008) and included the anterior prefrontal cortex (apFC: -36, 57, 3 and 36, 57, 3) and inferior parietal lobule (-44, -52, 54 and 48, -50, 52). Regions forming the motor network were based on Biswal et al. (1995) and included the left and right motor cortex (-42, -25, 63 and 42, -25, 63). All seed regions had a radius of 4 mm.

Finally, a measure of local functional coupling was calculated as described in detail elsewhere (Sepulcre et al., 2010; see also Tomasi and Volkow, 2010). Briefly, degree centrality is a network measure that quantifies the number of edges (or links) that are connected to a node in a graph (Rubinov and Sporns, 2010). Here brain voxels are the nodes and positive correlations between voxels  $>0.25$  are the links. Data were down sampled to 4 mm isotropic voxels. Local degree connectivity was calculated for each voxel by counting the number of links to other voxels within the immediate neighborhood (within a 12-mm radius). The output was a whole brain local degree connectivity map for each subject. For the present paper we took the *z*-transformed local degree connectivity map (with values ranging from 0 to 1; Buckner et al., 2009) of 50 young healthy subjects as published previously (Sepulcre et al., 2010) to create a binary mask of regions with high local degree connectivity ( $z > 0.75$ ). The metric of local functional coupling was the unstandardized average local degree

connectivity of all voxels within this mask. A high value for this metric means that the data show high local functional coupling.

We also computed for each subject a functional connectivity map representing the default network by correlating the mean signal time course from a spherical seed region within the posterior cingulate cortex (pCC; 4-mm radius; MNI coordinates 0, -53, 26; Van Dijk et al., 2010) with the time courses of all acquired voxels using Pearson's product moment correlation. Correlation maps were converted to *z*-maps using Fisher's *r*-to-*z* transformation. Group maps were computed by averaging the individual *z*(*r*) correlation maps.

## Results

#### Estimates of head motion

We explored the distribution of head motion across all 1088 usable subjects by plotting the frequency histogram of Mean Motion (the mean displacement of each brain volume as compared to the previous volume). A few observations are notable (Fig. 1A). First, there is substantial inter-subject variability. Second, a minority of subjects displayed disproportionately high levels of Mean Motion. Although this skewed distribution is expected from a distance measure it is worth noting that 8.5% of the subjects were outliers and 2.8% were extreme outliers when defined as Mean Motion greater than 2.0 and 2.5 standard deviations from the mean, respectively. Third, Mean Motion was lower for females than for males, which can be seen as a shift in their distributions ( $M_{\text{females}} = 0.048 \pm 0.020$ ,  $M_{\text{males}} = 0.054 \pm 0.025$ ,  $t(1086) = 5.33$ ,  $p < 0.001$ ). Comparing Mean Motion to the other three motion estimates revealed that all were correlated. Maximum Motion was the least stable metric with a moderate correlation to Mean Motion (Fig. 1B;  $r = 0.67$ ,  $p < 0.001$ ). This was not surprising because Maximum Motion is calculated based on a single image volume displacement for each subject. Mean Motion and Number of Movements were near proxies for one another (Fig. 1C;  $r = 0.96$ ,  $p < 0.001$ ), and Mean Motion and Rotation were strongly associated (Fig. 1D;  $r = 0.84$ ,  $p < 0.001$ ). Further analyses primarily used Mean Motion.

#### Head motion has a non-linear effect on temporal signal-to-noise

Fig. 2 plots the strong inverse relation between Mean Motion and tSNR, which suggests that subject motion introduces noise in the measurement. The relation was better modeled by non-linear regression ( $r = -0.61$ ,  $p < 0.001$ ) than linear regression ( $r = -0.57$ ,  $p < 0.001$ ). Here and elsewhere we display the quadratic regression term if it accounts for significant variance beyond the linear term. The subjects were divided into 10 groups ranging from those who moved least (Group 1) to those who moved most (Group 10). Mean Motion displacement per group is plotted by the black circles in Fig. 2 that fall along the non-linear curve fit.

#### Head motion is associated with decreased functional connectivity in large-scale networks

The central question of this paper is whether head motion is associated with differences in functional connectivity estimates. Mean Motion was found to systematically affect all four tested functional connectivity measures but not in the same direction. Analyses using Rotation were statistically indistinguishable. Increasing Mean Motion was associated with significantly decreased functional correlation strength among regions within the default network ( $r_{\text{linear}} = -0.18$ ,  $p < 0.001$ ; Fig. 3A) and the frontoparietal control network ( $r_{\text{linear}} = -0.16$ ,  $p < 0.001$ ; Fig. 3B). The plots and amount of variance accounted for by Mean Motion also revealed that head motion explains only a fraction of the variance across subjects, but that fraction may be critical and confound analyses.

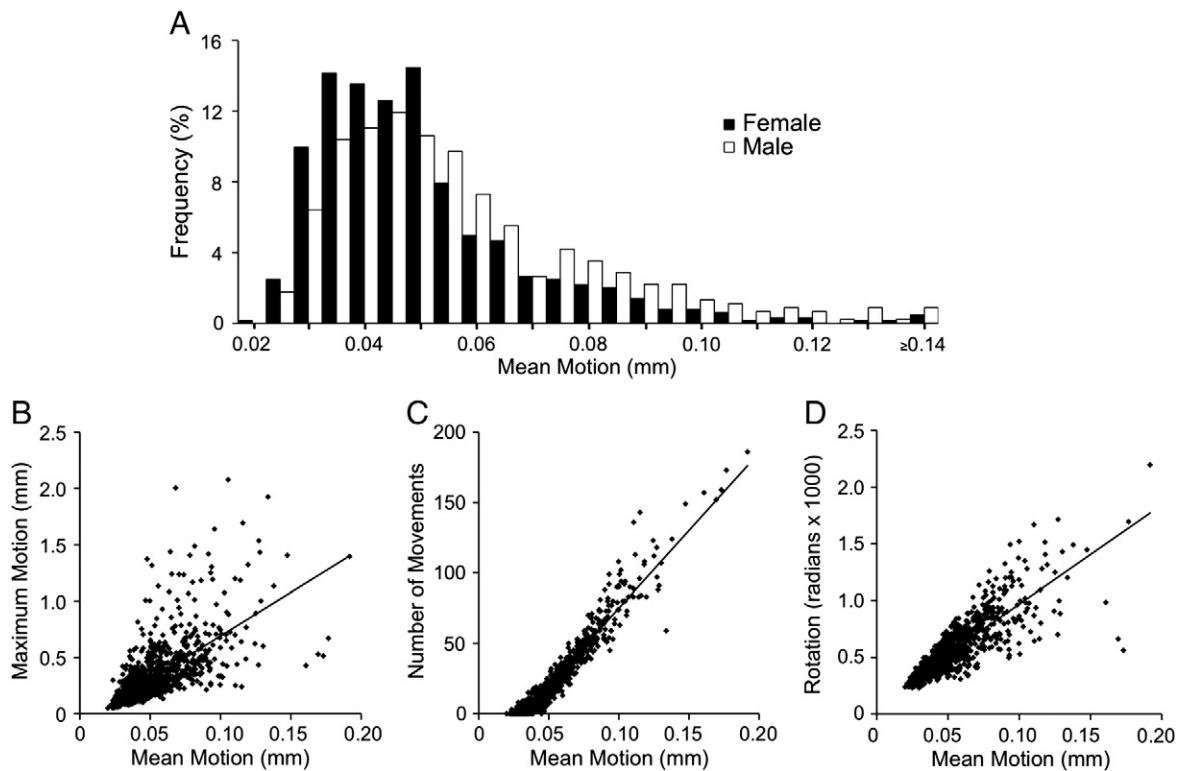


**Fig. 1.** Head motion estimates across subjects. (A) The frequency distribution of Mean Motion across the full sample ( $n=1088$ ). Mean Motion represents the mean absolute displacement of each brain volume as compared to the previous volume. Black bars represent females; white bars represent males. The distribution of motion for female subjects is shifted lower in relation to the male subjects. (B) The relation between Mean Motion and the Maximum Motion is illustrated. Each point represents a unique subject. The line plots linear regression ( $r=0.67$ ,  $p<0.001$ ). (C) The relation between Mean Motion and the Number of Movements between adjacent volumes  $>0.1$  mm ( $r=0.96$ ,  $p<0.001$ ). (D) The relation between Mean Motion and Rotation angle ( $r=0.84$ ,  $p<0.001$ ).

To illustrate the effects of head motion on functional connectivity, we constructed contrast maps between groups that differed in Mean Motion. Using a region in the posterior cingulate cortex as a seed we computed the functional connectivity map representing the default network for each subject. Contrasting Group 1 (10% of subjects that moved the least, Mean Motion = 0.027) with Group 10 (10% of subjects that moved the most, Mean Motion = 0.100) showed higher

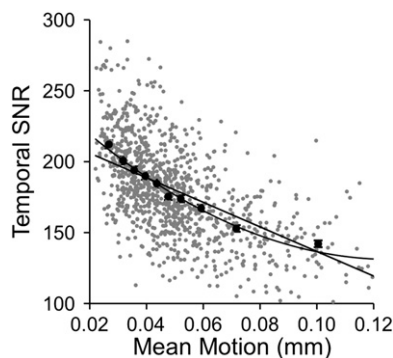


**Fig. 2.** Head motion is associated with reduced temporal signal-to-noise ratio (tSNR). The gray circles each represent a unique subject from a random sampling of 1000 subjects. There is a clear (expected) relation between Mean Motion and tSNR. The black line and curve represent the best linear ( $r=-0.57$ ,  $p<0.001$ ) and non-linear fit ( $r=-0.61$ ,  $p<0.001$ ) to the full sample of subjects. The black circles represent the mean values for each of 10 subgroups of subjects that were divided based on Mean Motion. Each black circle is from 100 subjects (10%) of the sample, so the leftmost circle is from the stillest 10% of the sample and the rightmost circle is from the 10% of the sample with the greatest head motion. Bars around the circles represent standard errors of the mean. The last two subgroups (20% of the sample) moved considerably more than the other eight subgroups, consistent with the skewed distribution apparent in Fig. 1.

functional connectivity in the low motion group throughout the default network including medial prefrontal cortex, lateral temporal cortex, and the inferior parietal lobule in the group that moved least (Fig. 4 left). A more moderate contrast between Groups 3 and 8 (Mean Motion = 0.036 and 0.059) also showed higher functional connectivity throughout the default network in the low motion group (Fig. 4 middle). Finally, contrasting Groups 5 and 6, with average motion parameters that are numerically very close but significantly different (Mean Motion = 0.044 and 0.048), yielded difference maps that resemble the canonical default network (Fig. 4 right). Thus, systematic but slight differences in head motion can produce functional connectivity differences.

#### Head motion increases local functional coupling

Head motion did not have the same effect on all functional connectivity measures. Increasing Mean Motion was associated with increased functional connectivity between the left and right motor regions ( $r_{linear}=0.07$ ,  $p<0.05$ ;  $r_{non-linear}=0.11$ ,  $p<0.005$ ) (Fig. 3C). In addition, increasing Mean Motion was associated with higher local functional coupling, i.e. connectivity to nearby regions ( $r_{linear}=0.09$ ,  $p<0.005$ ;  $r_{non-linear}=0.15$ ,  $p<0.001$ ; Fig. 3D). Thus, head motion can have systematically different effects on functional connectivity depending on the network and measure.

#### Between-subject head motion differences are stable

The considerable dispersion among head motion estimates in Fig. 1 raises the question of whether head motion varies from run to run or reflects a trait-like stable property of subjects. To explore this question, we examined the reliability of Mean Motion estimates

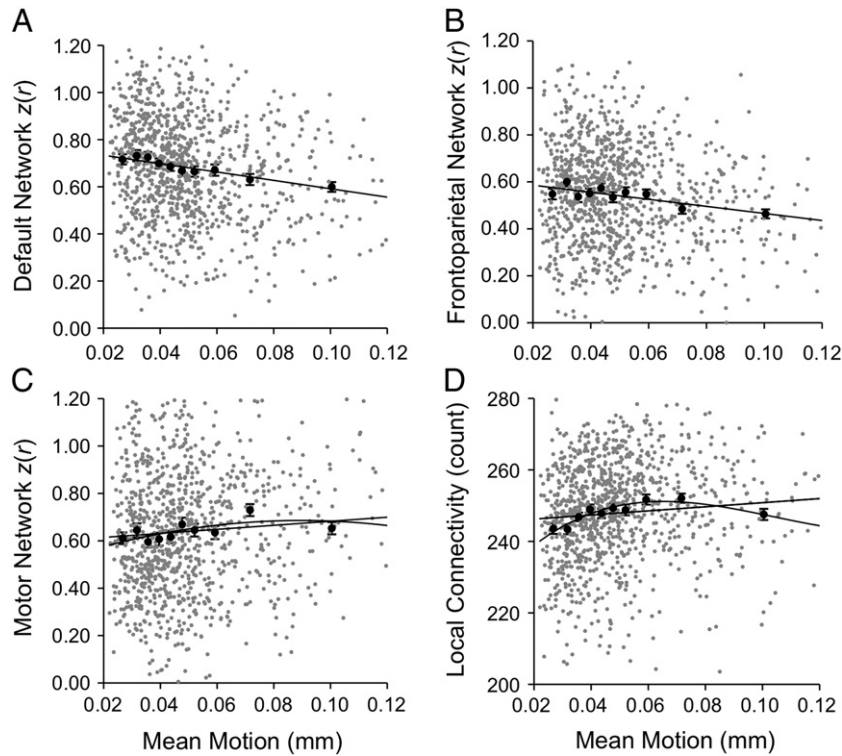


**Fig. 3.** Head motion is significantly correlated with functional connectivity but in opposing directions for distinct measures. Plot format parallels Fig. 2. (A) Functional correlation among regions within the default network shows a significant linear ( $r = -0.18, p < 0.001$ ) decrease with increasing Mean Motion. (B) Functional correlation among regions in the frontoparietal network also shows a significant linear decrease with increasing Mean Motion ( $r = -0.16, p < 0.001$ ). Non-linear regressions were not different from the linear fit. (C) Functional correlation between left and right motor regions shows a significant linear ( $r = 0.07, p = 0.026$ ) and non-linear ( $r = 0.11, p = 0.003$ ) increase with increasing Mean Motion. (D) Local functional coupling, a measure of functional connectivity to nearby voxels, also shows a significant linear ( $r = 0.09, p = 0.005$ ) and non-linear ( $r = 0.15, p < 0.001$ ) increase with increasing Mean Motion. The most extreme movers appear to show a decrease. The possibility of non-linear effects of head motion will be important to analysis strategies.

across independent scanning sessions in 42 subjects. Mean Motion was significantly correlated between the two sessions ( $r = 0.57, p < 0.001$  in the total sample;  $r = 0.66, p < 0.001$  when excluding four outliers) (Fig. 5), indicating that certain aspects of head motion may behave as a trait and present a potential confound when exploring individual differences within a population.

**Discussion**

The present study examined the influence of head motion on functional connectivity MRI. The primary result is that head motion has systematic effects on functional connectivity estimates that could easily be misinterpreted as neuronal effects. High levels of head

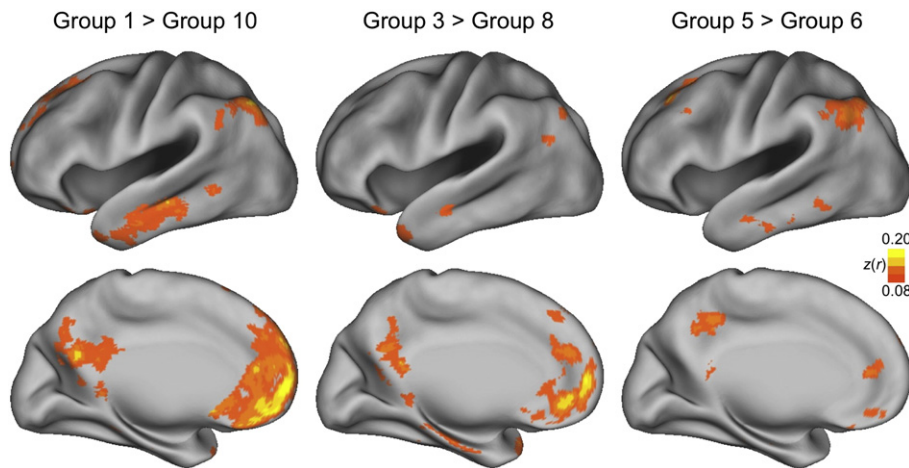


**Fig. 4.** Maps reveal functional connectivity network differences based solely on head motion. Group functional connectivity difference maps are presented to illustrate how head motion might confound an analysis. Each map represents the functional connectivity difference for one group of 100 subjects with lesser motion as compared to a second group with greater motion. Each map displays the surface projection for the difference for a seed region placed in the posterior cingulate. The leftmost image shows the contrast between the two most extreme groups (Group 1 is the stillest 10% of the subjects and Group 10 is the liveliest 10% of the subjects). Functional connectivity differences are observed throughout the default network including medial prefrontal cortex, lateral temporal cortex, and the inferior parietal lobule. The middle image shows a more moderate contrast between Groups 3 and 8. The rightmost image shows the contrast between Groups 5 and 6 that have Mean Motion estimates of 0.044 and 0.048 mm – an extremely subtle difference. Even in this tight range of motion, differences in head motion yield difference maps that could easily be mistaken for neuronal effects.

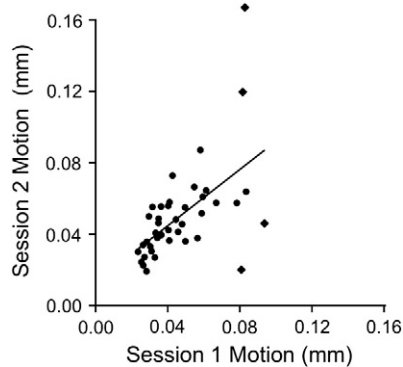


**Fig. 5.** Between-subject differences in head motion are stable. Mean Motion estimates are plotted for two separate scanning sessions conducted on separate days. Each data point represents a unique person. The correlation is significant ( $r=0.57$ ,  $p<0.001$ ) and increases further if the four outliers (denoted by diamonds) are removed ( $r=0.66$ ). Analyses of functional connectivity will need to consider the possibility that certain aspects of head motion behave as a trait and present a potential confound when exploring individual differences.

motion were associated with reduced functional connectivity in large-scale distributed networks (e.g., the default network and the frontoparietal control network; Figs. 3A and B) and increased local functional connectivity (Figs. 3C and D). Small differences in motion were sufficient to produce specific effects in seed-based functional connectivity maps (Fig. 4). Head motion was stable within individual subjects from one acquisition session to the next (Fig. 5) raising the possibility that motion can confound studies exploring individual differences within the same population.

### Implications

A clear implication of the present results is that it will be necessary to carefully consider the effects of head motion on functional connectivity MRI studies that examine individual differences or that contrast subject groups. A cursory literature review indicates that there are more than 100 studies that make such comparisons, many of which report between-group decreases in functional connectivity in distributed networks of brain regions. As an example of such a study, we examine one from our own laboratory – Andrews-Hanna et al. (2007). While that study did not examine functional correlations acquired at rest, it did contrast functional connectivity between subject groups during a continuous task state (a rapid event-related paradigm) that is presumably sensitive to the motion confounds reported here. It is thus a useful case study.

The primary finding of Andrews-Hanna et al. (2007) was robust reductions in functional connectivity across multiple large-scale brain networks (the default and dorsal attention networks) in healthy older adults relative to younger adults. The two groups differed in motion as calculated in the original study using a root-mean-squared estimate of motion that cumulated over the entire functional runs (young = 0.19 mm, old = 0.28 mm;  $p<0.001$ ). Examining the correlation between the posterior cingulate and the medial prefrontal cortex (one of the region pairs central to the paper) further reveals that the functional coupling estimate is influenced by motion. Subjects who moved more showed reduced functional connectivity across these two nodes of the default network ( $r=-0.47$ ,  $p<0.001$ ). When motion is regressed from the estimate of functional connectivity, the relation between age and functional coupling drops from  $r=0.71$  to  $r=0.54$  (remaining significant,  $p<0.001$ ). Thus, there is an effect of the motion estimate but it does not account for the major portion of the association.

However, it is still difficult to assess the full impact of motion. That study employed large non-isotropic voxels and any single motion metric is certainly imperfect. Residual components of motion may not

be captured. Also, the well-intended control analysis in the original report focused on local correlations within the visual system (which did not differ between groups). The assumption was that artifacts and motion would globally affect functional coupling between distributed regions. As the results in Fig. 3 reveal, head motion has different effects on different functional connectivity measures. Certain correlations between the hemispheres (Fig. 3C) and among local regions (Fig. 3D) increase with head motion. Thus, the original control is not sufficient in light of the present observation that motion has differential effects depending of the functional connectivity measure examined. We raise these points to make clear the complex challenges motion may have on between-group comparisons.

Beyond group comparisons, the present results also suggest that explorations of individual differences within the same population may be systematically affected by motion confounds. Fig. 5 illustrates that subjects who tend to move on one occasion tend to move on another occasion. Thus, head motion behaves like a trait and can be expected to influence individual subject estimates in ways that may yield systematic differences. This possibility should be carefully considered in genetic and heritability analyses.

We can place some boundary conditions on what to expect. While motion significantly and systematically affects functional connectivity estimates, the large variability of functional connectivity measures within motion groups, as shown in Fig. 3, reveals that the major portion of variance among people is not related to our present motion estimates. Recasting the data illustrated in Fig. 5 further clarifies this point. Head motion estimates are reliable ( $r=0.57$  in our present sample). The implication is that some portion (or all) of the reliable differences in functional connectivity measures might be attributable to motion. To explore this, we computed the test–retest reliability of four functional connectivity measures for the 42 subjects plotted in Fig. 5. The functional connectivity measures showed moderate reliability ( $r=0.61$ , 0.66, 0.43 and 0.44 for the default network, frontoparietal control, motor network, and local functional coupling, respectively). When head motion was regressed from the estimates, the test–retest reliability remained at about the same level ( $r=0.68$ , 0.62, 0.43, and 0.46, respectively). Thus, head motion does not seem to account for the major portion of stable between-subject variation in functional connectivity.

Nonetheless, it is important not to underestimate the challenge of head motion. Head motion is a particularly insidious confound. It is insidious because it biases between-group studies often in the direction of the hypothesized difference. Given that different populations have different data artifacts and levels of motion, and further that head motion does not affect all functional connectivity estimates in a similar fashion, it will be important to address the confound of motion on a case by case basis. That is, even though there is considerable variation that is not due to head motion, in any given instance, a between-group difference could be entirely due to motion. Paradoxically, large data samples may be particularly vulnerable to this kind of confound where small, systematic differences in motion could become the dominant difference as other sources of variation are matched between groups. The rightmost panel of Fig. 4 illustrates this point. The panel compares two large samples (each  $n=100$ ) that were matched for age and sex but systematically differed in a small degree of motion (0.044 versus 0.048 mm Mean Motion displacement). A between-group effect on functional connectivity of the default network is evident that is most likely entirely driven by head motion. This difference in another context could easily be mistaken for a true neuronal effect.

### Potential ways to address head motion

Confronting motion artifacts is not a new challenge for the field and several potential causes of motion have been identified. Gross motion may arise from shifts in head position during the scan or from

swallowing and jaw clenching; cardiac cycles and respiration are also known to contribute to motion artifacts (Birn et al., 2008a; Enzmann and Pelc, 1992; Glover et al., 2000; Huettel et al., 2004). Findings from task-based fMRI studies suggest that motion may be more strongly related to subject groups than to properties of the task itself (Seto et al., 2001), which is consistent with our finding that head motion behaves – to some degree – as a subject-specific trait. We suspect that the major portion of the head motion affecting functional connectivity in our analyses is due to gross head movement in space and, specifically, head motion that persists after within-subject motion correction and regression of non-specific signals from white-matter and CSF. The opposing effects of decreased and increased functional connectivity may be caused by spatial blurring due to motion. Spatial blurring will increase local correlation of the signal while decreasing the strength of long-range coupling to anatomically-specific regions. One exception might be distant coupling between bilateral brain regions, such as the motor cortex, that could be exposed to symmetric movements of the homologous region pairs.

Multiple strategies have the potential to address the challenge of head motion in studies using functional connectivity that are as simple as better procedures for head immobilization and careful instruction (and reminding) about the importance of staying still. One interesting approach by Yang et al. (2005) involved real time feedback to indicate when movement exceeded a specified threshold. Head immobilization and instruction will only go so far to mitigate the challenge as cardiac cycles, respiration, and involuntary movements such as swallowing will persist under the best circumstances. Other strategies to address motion might include approaches that (1) improve traditional nuisance regression techniques (for a recent example see Jo et al., 2010), (2) prospectively correct for motion during data acquisition (Thesen et al., 2000; Ward et al., 2000), (3) post-hoc eliminate images or epochs where motion is evident (Power et al., 2011), (4) regress physiological signals associated with cardiac and respiratory motion either directly measured (e.g. Birn et al., 2008b; Chang et al., 2009) or as estimated from the data itself (e.g. Beall and Lowe, 2007, 2010), (5) regress motion estimates from between-subject analyses, and (6) match the level of motion between subject groups.

## Conclusions

Head motion significantly affects measures of functional connectivity MRI even within the range of motion exhibited by typical, healthy young adults. The effects are dependent on the specific measure and include decreased functional coupling for distributed networks and increased functional coupling for local networks. Since motion was found to be a stable property within subjects – behaving as a trait – studies of genetic associations, heritability, and relations to behavior and personality will all need to consider the influence of head motion. Analyses that contrast groups that differ in their tendency to move will be particularly vulnerable to the confounding effects of motion, especially when the group more likely to move shows reductions in distributed and increases in local functional coupling (e.g., children and older adults). Application of strategies to reduce motion and sophisticated methods to regress physiological signals associated with cardiac and respiratory motion may prove beneficial for studies contrasting groups that systematically differ in terms of head motion during the scan.

## Acknowledgments

We thank the Harvard Center for Brain Science Neuroimaging Core, the Athinoula A. Martinos Center for imaging support, and the Harvard Neuroinformatics Research Group (Gabriele Fariello, Timothy O'Keefe, and Victor Petrov). The data analyzed were collected as part of the Genomics Superstruct Project. We thank Marisa Hollinshead, Elizabeth Hemphill, Leah Bakst, Angela Castellanos, and Sara Ruben-

stein for assistance in collecting the data. Avram Holmes and Jorge Sepulcre assisted in constructing the functional connectivity measures, and Avi Snyder provided valuable discussion. This work was supported by NIA Grants (AG021910, P41RR14074, K08MH067966), the Howard Hughes Medical Institute, and the Simons Foundation. Dr. Sabuncu receives support from a KL2 Medical Research Investigator Training (MeRIT) grant awarded via Harvard Catalyst, The Harvard Clinical and Translational Science Center (NIH grant 1KL2RR025757 and financial contributions from Harvard University and its affiliated academic health care centers).

## References

- Andrews-Hanna, J.R., Snyder, A.Z., Vincent, J.L., Lustig, C., Head, D., Raichle, M.E., Buckner, R.L., 2007. Disruption of large-scale brain systems in advanced aging. *Neuron* 56, 924–935.
- Beall, E.B., Lowe, M.J., 2007. Isolating physiologic noise sources with independently determined spatial measures. *NeuroImage* 37, 1286–1300.
- Beall, E.B., Lowe, M.J., 2010. The non-separability of physiologic noise in functional connectivity MRI with spatial ICA at 3T. *J. Neurosci. Methods* 191, 263–276.
- Birn, R.M., Murphy, K., Bandettini, P.A., 2008a. The effect of respiration variations on independent component analysis results of resting state functional connectivity. *Hum. Brain Mapp.* 29, 740–750.
- Birn, R.M., Smith, M.A., Jones, T.B., Bandettini, P.A., 2008b. The respiration response function: the temporal dynamics of fMRI signal fluctuations related to changes in respiration. *NeuroImage* 40, 644–654.
- Biswal, B., Yetkin, F.Z., Haughton, V.M., Hyde, J.S., 1995. Functional connectivity in the motor cortex of resting human brain using echo-planar MRI. *Magn. Reson. Med.* 34, 537–541.
- Buckner, R.L., 2010. Human functional connectivity: new tools, unresolved questions. *Proc. Natl. Acad. Sci. U. S. A.* 107, 10769–10770.
- Buckner, R.L., Sepulcre, J., Talukdar, T., Krienen, F.M., Liu, H., Hedden, T., Andrews-Hanna, J.R., Sperling, R.A., Johnson, K.A., 2009. Cortical hubs revealed by intrinsic functional connectivity: mapping, assessment of stability, and relation to Alzheimer's disease. *J. Neurosci.* 29, 1860–1873.
- Chang, C., Cunningham, J.P., Glover, G.H., 2009. Influence of heart rate on the BOLD signal: the cardiac response function. *NeuroImage* 44, 857–869.
- Cole, D.M., Smith, S.M., Beckmann, C.F., 2010. Advances and pitfalls in the analysis and interpretation of resting-state fMRI data. *Front. Syst. Neurosci.* 4, 8.
- Enzmann, D.R., Pelc, N.J., 1992. Brain motion: measurement with phase-contrast MR imaging. *Radiology* 185, 347–353.
- Evans, A.C., Collins, D.L., Mills, S.R., Brown, E.D., Kelly, R.L., Peters, T.M., 1993. 3D statistical neuroanatomical models from 305 MRI volumes. *Proceedings of IEEE-Nuclear Science Symposium and Medical Imaging Conference*, pp. 1813–1817.
- Fornito, A., Bullmore, E.T., 2010. What can spontaneous fluctuations of the blood oxygenation-level-dependent signal tell us about psychiatric disorders? *Curr. Opin. Psychiatry* 23, 239–249.
- Fornito, A., Zalesky, A., Bassett, D.S., Meunier, D., Ellison-Wright, I., Yucel, M., Wood, S.J., Shaw, K., O'Connor, J., Nertney, D., Mowry, B.J., Pantelis, C., Bullmore, E.T., 2011. Genetic influences on cost-efficient organization of human cortical functional networks. *J. Neurosci.* 31, 3261–3270.
- Fox, M.D., Greicius, M., 2010. Clinical applications of resting state functional connectivity. *Front. Syst. Neurosci.* 4, 19.
- Glahn, D.C., Winkler, A.M., Kochunov, P., Almasy, L., Duggirala, R., Carless, M.A., Curran, J.C., Olvera, R.L., Laird, A.R., Smith, S.M., Beckmann, C.F., Fox, P.T., Blangero, J., 2010. Genetic control over the resting brain. *Proc. Natl. Acad. Sci. U. S. A.* 107, 1223–1228.
- Glover, G.H., Li, T.Q., Ress, D., 2000. Image-based method for retrospective correction of physiological motion effects in fMRI: RETROICOR. *Magn. Reson. Med.* 44, 162–167.
- Honey, C.J., Sporns, O., Cammoun, L., Gigandet, X., Thiran, J.P., Meuli, R., Hagmann, P., 2009. Predicting human resting-state functional connectivity from structural connectivity. *Proc. Natl. Acad. Sci. U. S. A.* 106, 2035–2040.
- Huettel, S.A., Song, A.W., McCarthy, G., 2004. *Functional Magnetic Resonance Imaging*, First Edition. Sinauer Associates, Sunderland, MA.
- Jenkinson, M., Bannister, P., Brady, M., Smith, S., 2002. Improved optimization for the robust and accurate linear registration and motion correction of brain images. *NeuroImage* 17, 825–841.
- Jo, H.J., Saad, Z.S., Simmons, W.K., Milbury, L.A., Cox, R.W., 2010. Mapping sources of correlation in resting state fMRI, with artifact detection and removal. *NeuroImage* 52, 571–582.
- Kwong, K.K., Belliveau, J.W., Chesler, D.A., Goldberg, I.E., Weisskoff, R.M., Poncelet, B.P., Kennedy, D.N., Hoppel, B.E., Cohen, M.S., Turner, R., et al., 1992. Dynamic magnetic resonance imaging of human brain activity during primary sensory stimulation. *Proc. Natl. Acad. Sci. U. S. A.* 89, 5675–5679.
- Meindl, T., Teipel, S., Elmouden, R., Mueller, S., Koch, W., Dietrich, O., Coates, U., Reiser, M., Glaser, C., 2010. Test-retest reproducibility of the default-mode network in healthy individuals. *Hum. Brain Mapp.* 31, 237–246.
- Ogawa, S., Tank, D.W., Menon, R.S., Ellermann, J.M., Kim, S.G., Merkle, H., Ugurbil, K., 1992. Intrinsic signal changes accompanying sensory stimulation: functional brain mapping with magnetic resonance imaging. *Proc. Natl. Acad. Sci. U. S. A.* 89, 5951–5955.

- Power, J.D., Barnes, K.A., Snyder, A.Z., Schlaggar, B.L., Petersen, S.E., 2011. Spurious but systematic correlations in resting state functional connectivity MRI arise from head motion. *Soc. Neurosci. Abstr.* 290.03.
- Raichle, M.E., MacLeod, A.M., Snyder, A.Z., Powers, W.J., Gusnard, D.A., Shulman, G.L., 2001. A default mode of brain function. *Proc. Natl. Acad. Sci. U. S. A.* 98, 676–682.
- Rubinov, M., Sporns, O., 2010. Complex network measures of brain connectivity: uses and interpretations. *NeuroImage* 52, 1059–1069.
- Sepulcre, J., Liu, H., Talukdar, T., Martincorena, I., Yeo, B.T., Buckner, R.L., 2010. The organization of local and distant functional connectivity in the human brain. *PLoS Comput. Biol.* 6, e1000808.
- Seto, E., Sela, G., McLroy, W.E., Black, S.E., Staines, W.R., Bronskill, M.J., McIntosh, A.R., Graham, S.J., 2001. Quantifying head motion associated with motor tasks used in fMRI. *NeuroImage* 14, 284–297.
- Shehzad, Z., Kelly, A.M.C., Reiss, P.T., Gee, D.G., Gotimer, K., Uddin, L.Q., Lee, S.H., Margulies, D.S., Roy, A.K., Biswal, B.B., Petkova, E., Castellanos, F.X., Milham, M.P., 2009. The resting brain: unconstrained yet reliable. *Cereb. Cortex* 19, 2209–2229.
- Thesen, S., Heid, O., Mueller, E., Schad, L.R., 2000. Prospective acquisition correction for head motion with image-based tracking for real-time fMRI. *Magn. Reson. Med.* 44, 457–465.
- Tomasi, D., Volkow, N.D., 2010. Functional connectivity density mapping. *Proc. Natl. Acad. Sci. U. S. A.* 107, 9885–9890.
- Van der Kouwe, A.J., Benner, T., Fischl, B., Schmitt, F., Salat, D.H., Harder, M., Sorensen, A.G., Dale, A.M., 2005. On-line automatic slice positioning for brain MR imaging. *NeuroImage* 27, 222–230.
- Van der Kouwe, A.J., Benner, T., Salat, D.H., Fischl, B., 2008. Brain morphometry with multiecho MPRAGE. *NeuroImage* 40, 559–569.
- Van Dijk, K.R.A., Hedden, T., Venkataraman, A., Evans, K.C., Lazar, S.W., Buckner, R.L., 2010. Intrinsic functional connectivity as a tool for human connectomics: theory, properties, and optimization. *J. Neurophysiol.* 103, 297–321.
- Vincent, J.L., Snyder, A.Z., Fox, M.D., Shannon, B.J., Andrews, J.R., Raichle, M.E., Buckner, R.L., 2006. Coherent spontaneous activity identifies a hippocampal–parietal memory network. *J. Neurophysiol.* 96, 3517–3531.
- Vincent, J.L., Kahn, I., Snyder, A.Z., Raichle, M.E., Buckner, R.L., 2008. Evidence for a frontoparietal control system revealed by intrinsic functional connectivity. *J. Neurophysiol.* 100, 3328–3342.
- Vogel, A.C., Power, J.D., Petersen, S.E., Schlaggar, B.L., 2010. Development of the brain's functional network architecture. *Neuropsychol. Rev.* 20, 362–375.
- Ward, H.A., Riederer, S.J., Grimm, R.C., Ehman, R.L., Felmlee, J.P., Jack Jr., C.R., 2000. Prospective multiaxial motion correction for fMRI. *Magn. Reson. Med.* 43, 459–469.
- Yang, S., Ross, T.J., Zhang, Y., Stein, E.A., Yang, Y., 2005. Head motion suppression using real-time feedback of motion information and its effects on task performance in fMRI. *NeuroImage* 27, 153–162.
- Yeo, B.T.T., Krienen, F.M., Sepulcre, J., Sabuncu, M.R., Lashkari, D., Hollinshead, M., Roffman, J.L., Smoller, J.W., Zollei, L., Polimeni, J.R., Fischl, B., Liu, H., Buckner, R.L., 2011. The organization of the human cerebral cortex estimated by functional connectivity. *J. Neurophysiol.* doi:10.1152/jn.0038.2011.
- Zar, J.H., 1996. *Biostatistical Analysis*. Prentice Hall, Upper Saddle River NJ.
- Zhang, D., Raichle, M.E., 2010. Disease and the brain's dark energy. *Nat. Rev. Neurol.* 6, 15–28.
- Zuo, X.N., Di Martino, A., Kelly, C., Shehzad, Z.E., Gee, D.G., Klein, D.F., Castellanos, F.X., Biswal, B.B., Milham, M.P., 2010. The oscillating brain: complex and reliable. *NeuroImage* 49, 1432–1445.